Experimental realization of sonic demultiplexing devices based on inverse designed scattering acoustic elements

Andreas Håkansson, José Sánchez-Dehesa,[a] and Francisco Cervera
Wave Phenomena Group, Nanophotonics Technology Center, Polytechnic University of Valencia, C/Camino de Vera s/n, E-46022 Valencia, Spain

(Received 19 December 2005; accepted 8 March 2006; published online 18 April 2006)

We present experiments demonstrating sonic demultiplex devices able to separate spatially several wavelengths. The devices are based on clusters of circular scatterers whose position and size are determined by using an inverse design approach. Two prototypes are built and characterized, a first that spatially separates two wavelengths (i.e., 20.0 and 22.7 cm) and a second that separates three wavelengths: 20.0, 21.3, and 22.7 cm. Both prototypes are typical examples of acoustic scattering elements, a name here introduced to define inverse designed devices that are characterized by their great adaptability in controlling the scattering image, including both the reflected and transmitted waves. © *2006 American Institute of Physics*. [DOI: 10.1063/1.2196867]

Inverse design is commonly used to generate diffractive optical elements[1,2] (DOEs), which are optical devices used to fulfill a given functionality. They consist of an array of elements on a plane (layer), where each element manipulates the phase of a part of some external incident light beam. This manipulation can be addressed by a parameter that controls the light passing through that specific element. Setting all parameters will correspond to one complete image of the light passing (or reflected by) the DOE, reconstructed through destructive and constructive interference.

Scattering optical elements (SOEs) were recently proposed[3] and do not only rely on single layer arrays but on multiple layers of two-dimensional (2D) scattering objects. The introduction of a new dimension of freedom leads to a higher level of control. The SOEs do not only take into account the phase of the dispersed waves but also the full complex scattering process. The nature of waves makes it possible to transfer the underlying physics of SOEs from light to sound. Note that this transfer is not possible for transparent DOEs due to the high acoustic impedance of solids. Here, we will show how the scattering of sound can be controlled by inverse designed scattering acoustical elements (SAEs), a name that defines the acoustic counterparts of SOEs. Several transparent acoustical devices have been proposed till now, but they are mostly based on the properties of periodic distributions of sound scatterers in air; focusing devices based on standard refraction[4] or negative refraction,[5] interferometers,[6] and collimating[7] and mode-selecting[8] devices are only a few examples.

This letter presents the experimental realization of two inverse designed acoustic devices that accomplish the spatial separation of acoustic signals carrying up to three different wavelengths. They are based on 2D arrangements of rigid cylinders in air. These devices and the acoustical lenses recently proposed[9] and demonstrated[10] are typical examples of SAEs.

To perform the inverse design process, first the direct problem (i.e., the scattering of an acoustic wave by a fixed configuration of 2D scatterers) needs to be solved. We use multiple scattering theory[11] (MST) to simulate this process. This approach has been used earlier[6,10,12] to simulate similar structures and a very good agreement with experiments were obtained. Furthermore, a genetic algorithm[13] (GA) has been implemented to optimize the parameters of this SAE, i.e., the cylinders' positions and their diameters. The analogous MST-GA inverse design approach was previously introduced in photonics.[14]

Figures 1(a) and 1(b) give, respectively, artistic and schematic views of the setup problem. The proposed SAE is located inside the region defined by the dashed lines and consists of a cluster of cylindrical rods with different radii. A sound source, S, isotropically emits sound containing several wavelengths. The plot represents a particular wavelength that

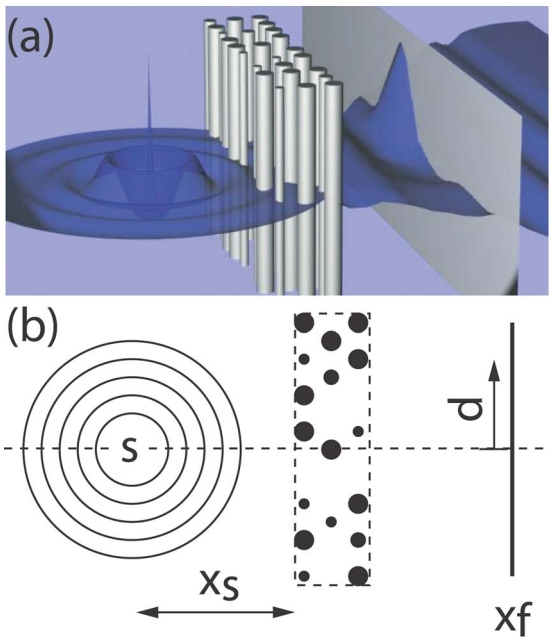

FIG. 1. (Color online) (a) An artistic and (b) a schematic view of the scattering acoustical element (SAE) setup. The incident wave (S) is shown at the right of the SAE, which consists of an array of cylinders enclosed in the region defined by the dashed lines. The letters in (b) define the parameters used in the inverse design process.

[a]Author to whom correspondence should be addressed; electronic mail: jsdehesa@upvnet.upv.es

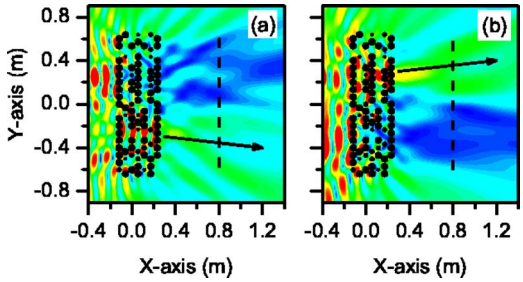

FIG. 2. (Color online) Calculated pressure maps $[|P_\lambda(x,y)|]$ for the scattering of a sound plane wave (with wavelength λ) by a scattering acoustical element that acts as a two wavelength demultiplexing device (black dots). (a) Map associated with the wave $\lambda_1=20.0$ cm. (b) Map associated with $\lambda_2=22.7$ cm. The arrows are guides for the eye and define the flow of transmitted wavelength. The vertical dashed lines define the plane x_f in Fig. 1.

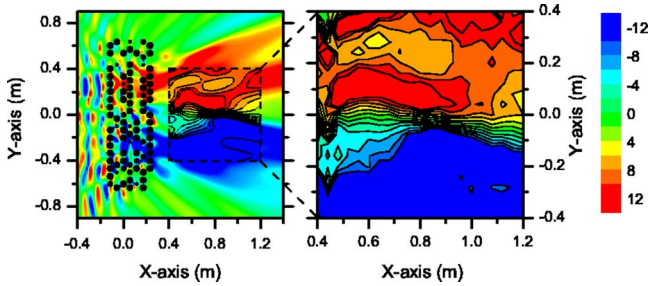

FIG. 3. (Color online) These maps depict the function $-20\log(|P_{\lambda_1}(x,y)|/|P_{\lambda_2}(x,y)|)$ for the optimized seven layer SAE (black dots). (Left panel) Map obtained by multiple scattering simulations. (Right panel) Map experimentally obtained by measurements performed inside the area enclosed by the dashed lines in the left panel. The black lines define levels of equal pressure; the difference between two adjacent levels is 2 dB.

after scattering by the cluster deviated a distance d at the white plane in Fig. 1(a) and by x_f in Fig. 1(b).

To generate the first demultiplexing device (i.e., the one producing the spatial separation of only two wavelengths) we defined a hexagonal array with parameter $a=6.70$ cm as possible lattice sites (LSs) for the cylindrical rods. The total width of the device was fixed to $19a=1.27$ m. Rods with three different diameters (ϕ) were considered in the design process, $\phi=2,3,4$ cm. This results in 2 bit parameters coding the device, each parameter representing one of the four different scatterers (including vacant) at each LS, which is fixed during the optimization process. Furthermore, the objective function [referred to the fitness in GAs (Ref. 13)] to be maximized was set to

$$f_1(\mathbf{s})(\text{in dB}) = 20\log\left(\int_{y=-d}^{y=0}\frac{|P_{\lambda_2}(x_f,y)|}{|P_{\lambda_1}(x_f,y)|}dy \times \int_{y=0}^{y=d}\frac{|P_{\lambda_1}(x_f,y)|}{|P_{\lambda_2}(x_f,y)|}dy\right), \quad (1)$$

where $\mathbf{s}$ is a vector including all parameters coding the SAE (chromosome) and $|P_\lambda(x,y)|$ is the pressure modulus for a fixed wavelength λ.

Various designs were optimized with different numbers of layers. In general, the larger the number of layer, the higher the maximized fitness. Here, a seven layer device is presented to illustrate the two wavelength demultiplexing functionality. This device corresponds to 136 different fixed LSs in the hexagonal frame, which result in a $136\times 2=272$ bit optimization problem. In other words $\mathbf{s}$ in Eq. (1) corresponds to a 272 bit string coding all parameters of the SAE. The designed device is depicted in Figs. 2 and 3 by black dots. It was obtained by maximizing f_1, where parameters x_f and d were set to 0.8 m and 0.6 m, respectively, and wavelengths λ_1 and λ_2 were chosen to be 20.0 and 22.7 cm. Simulated pressure maps in Figs. 2(a) and 2(b) give an accurate view of the wavelength demultiplex functionality that can clearly be spotted by the large blue areas, which correspond to low intensity sound. Sound with a wavelength λ_1 (λ_2) is clearly directed to the lower (upper) right. Figure 3(a) shows the predicted difference in decibels between the two distinctive signals. These values are related to the crosstalk between the two channels. Positive values (red) correspond to areas where λ_2 dominates over λ_1 and negative values (blue) mark the opposite relation. The two regions are clearly separated by the plane at $y=0.0$ m, as was the preset criterion of the design. The wavelength division functionality is observed in a large area.

The SAE prototype was constructed by using 2 m long aluminum bars as sound scatterers that were placed in position by hanging them to a frame with hexagonal symmetry. Finally, the incident signal was produced by a column speaker separated approximately 2 m from the SAE. The characterization was performed in an anechoic chamber by using the same experimental setup described in Ref. 10. Figure 3(b) shows the measurements obtained in a small area near the SAE. Notice that the agreement with simulation is not only qualitative but also quantitative.

To achieve a three wavelength demultiplexing device, the number of layers had to be increased from 7 to 9, which corresponds to an increase from 136 to 175 LSs, resulting in a 350 bit optimization problem. The two extra layers were added to the left hand side of the structure, keeping the distance between $x_f=0.8$ m and the outer layer of the device constant. The new objective function was set to

$$f_2(\mathbf{s})(\text{in dB}) = 20\log\left(\int_{-d}^{-d/3}\frac{|P_{\lambda_1}(y)|}{|P_{\lambda_2}(y)|+|P_{\lambda_3}(y)|} \times \int_{-d/3}^{d/3}\frac{|P_{\lambda_3}(y)|}{|P_{\lambda_1}(y)|+|P_{\lambda_2}(y)|} \times \int_{d/3}^{d}\frac{|P_{\lambda_2}(y)|}{|P_{\lambda_1}(y)|+|P_{\lambda_3}(y)|}\right). \quad (2)$$

The employed parameters are equal to those of the first design and the third wavelength (λ_3) is chosen between the two used earlier, i.e., $\lambda_1=20.0$ cm, $\lambda_2=22.7$ cm, and $\lambda_3=21.3$ cm. Notice that the spatial distribution of each channel is reduced to $2d/3$ to fit in all three channels.

Figure 4 shows the optimized device and its predicted functionality. The simulation indicates that a fully working device with the asked-for features is realistic. Each port shows an averaged crosstalk of -6 dB. The prototype was constructed and characterized as for the seven layer device. Figure 5 shows a comparison between measurements (symbols) and simulations (lines), both taken at the plane of projection, x_f. An excellent agreement between theory and experiment is still achieved, even though the number of scatterers has been increased. At this point it is interesting to remark that in comparison with previous experiments,[10]

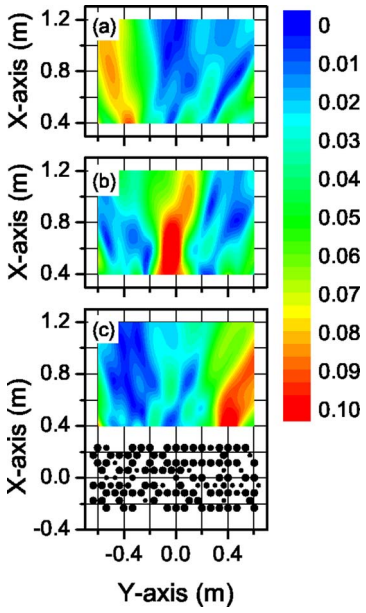

FIG. 4. (Color online) Three wavelength demultiplex SAE. The figure illustrates three maps of the transmitted pressure (the sound impinges the SAE from the bottom). Each map corresponding to one wavelength: (a) 20.0 cm, (b) 21.3 cm, and (c) 22.7 cm. The color scale used goes from red (high amplitude) via green to blue (low amplitude). The black dots show a schematic view of the nine layer SAE device.

where an increasing number of layers reduced the predicted performance of the designed device, now the agreement with simulations is maintained. An analysis of the different setups lets us to conclude that the origin of the obtained improvement is due to the sound source, which here is easily simulated by a line sonic source.

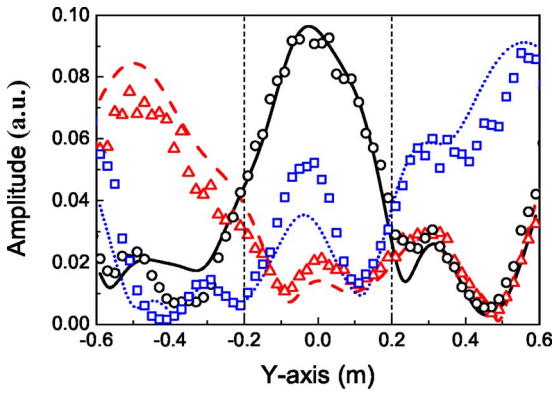

FIG. 5. (Color online) Experimental characterization of a three wavelength demultiplex SAE. The symbols mark the measured pressure amplitudes and the solid lines define those obtained by multiple scattering simulations, for a cross section at x_f=0.8 m. The three colors (symbols), blue (squares), black (circles), and red (triangles), correspond to the three spatially separated wavelengths, 22.7, 21.3, and 20.0 cm, respectively.

In summary, we have shown that a cluster of discrete scatterers, so called SAE, can be inverse designed to wavelength demultiplex an incident acoustic wave. We have positively characterized a three wavelength demultiplex SAE prototype using nine layers of cylindrical scatterers as well as a seven layer SAE separating two wavelengths. Devices that spatially separate sound with several wavelengths are of interest for applications in ultrasonic spectroscopy,[15] for example, to explore simultaneously velocity fluctuations in fluidized suspensions of particles in separated regions. Frequency controlled beam steering should be also possible by these devices, a property that could be applied to develop ultrasonic actuators.[16] These results give an insight into the great spectra of possible devices for molding the flow of sound.

This work was partially supported by the Spanish Ministry of Science and Education (Project No. TEC2004-03545). One of the authors (A.H.) acknowledges his Ph.D. grant paid by Nanophotonic Technology Center of Valencia. The authors thank Professor J. Llinares and Dr. F. Meseguer for their permanent support. The technical facilities provided by the group ACARMA at the UPV are also gratefully acknowledged.

[1] L. B. Lesem, P. M. Hirsch, and J. A. Jordan, Jr., IBM J. Res. Dev. **13**, 150 (1969).
[2] J. L. Horner and P. D. Gianino, Appl. Opt. **23**, 812 (1984).
[3] A. Håkansson and J. Sánchez-Dehesa, Appl. Phys. Lett. **87**, 193506 (2005).
[4] F. Cervera, L. Sanchis, J. V. Sánchez-Pérez, R. Martinez-Sala, C. Rubio, F. Meseguer, C. López, D. Caballero, and J. Sánchez-Dehesa, Phys. Rev. Lett. **88**, 023902 (2002).
[5] Suxia Yang, J. H. Page, Zhengyou Liu, M. L. Cowan, C. T. Chan, and Ping Sheng, Phys. Rev. Lett. **93**, 024301 (2004).
[6] L. Sanchis, A. Håkansson, F. Cervera, and J. Sánchez-Dehesa, Phys. Rev. B **67**, 035422 (2003).
[7] Chunyin Qiu, Zhengyou Liu, Jing Shi, and C. T. Chan, Appl. Phys. Lett. **86**, 224105 (2005).
[8] Chunyin Qiu, Zhengyou Liu, Jun Mei, and Jing Shi, Appl. Phys. Lett. **87**, 104101 (2005).
[9] A. Håkansson, J. Sánchez-Dehesa, and L. Sanchis, Phys. Rev. B **70**, 214302 (2004).
[10] A. Håkansson, F. Cervera, and J. Sánchez-Dehesa, Appl. Phys. Lett. **86**, 054104 (2005).
[11] A. Ishimaru, *Electromagnetic Wave Propagation, Radiation, and Scattering* (Prentice-Hall, NJ, 1991).
[12] B. C. Gupta and Z. Ye, Phys. Rev. E **67**, 036603 (2003).
[13] D. E. Goldberg, *Genetic Algorithms in Search, Optimization and Learning* (Addison-Wesley, Reading, MA, 1989).
[14] L. Sanchis, A. Håkansson, D. Lopez-Zanón, J. Bravo-Abad, and J. Sánchez-Dehesa, Appl. Phys. Lett. **84**, 4460 (2004).
[15] M. L. Cowan, J. H. Page, and D. A. Weitz, Phys. Rev. Lett. **85**, 453 (2000).
[16] J. Hu, C. Tay, Y. Cai, and J. Du, Appl. Phys. Lett. **87**, 094104 (2005).